

# Experimental Study of the Influence of the Rotor Dimensions on the Performances of Solid Rotor Asynchronous Motor

HACHEMI MABROUK<sup>1</sup>, ABDESSEMED RACHID<sup>2</sup>

<sup>1</sup> Laboratory of Automatics of Setif (LAS), Department of Electrotechnics,  
Faculty of Engineering, University of Setif, ALGERIA

<sup>2</sup> Department of Electrotechnics, Faculty of Engineering,  
University of Batna, ALGERIA

---

**Abstract:** - This paper presents an experimental investigation on the effect of the rotor geometry on the performances of a solid rotor asynchronous motor. The practical tests have been done on six solid rotors (2 smooth and 4 grooved) by varying: the smooth rotors diameter, the grooves number, the grooves depth (constant grooves width), the grooves width (constant grooves depth). The experimental results are exposed by considering two essential parameters: electromagnetic torque and the power factor for different supply voltage.

**Key-Words:** Asynchronous motor, smooth solid rotor, grooved solid rotor, geometry, experimental study.

## 1 Introduction

The solid rotor asynchronous motors adapt well to the industrial applications of high powers requiring high speeds [1],[2]. The advancement of technology is very closely associated with the increase of operations speeds in almost all the branches of the industry. Increasing the speeds result in an increase in productivity, quality of production and accuracy of working. The high speed electrical motors find their applications in machine tools industry, in gyroscopic applications...etc. Therefore, they become very important to improve the electrical performances of a solid rotor motors to make it commercially viable for use in industrial applications.

The improvement in the solid rotor motor characteristics is often suggested by methods such as: extended rotor; providing end rings of highly conducting material, such as copper or brass; by depositing the layers of copper, iron and cobalt (Cu+(Fe-Co)) and copper, iron and Nickel (Cu+(Fe-Ni)), in few tens of microns; by making grooves parallel to the axis of the solid rotor [2],[3]. The solid rotor structure, presenting a great mechanical security, allows achieving asynchronous motors for very high speeds. The smooth solid rotor asynchronous motor was the object of several studies [4], [5]. This motor has a best starting torque than the classic asynchronous motor (squirrel cage), but its electrical characteristics deteriorate considerably for the weak slips and the reasons are at a time electric and magnetic. The rotor currents

close before reaching the rotor extremities and the stator flux does not penetrate deeply in the rotor. In contrast to the smooth solid rotor, the grooved rotor presents a very complex geometry.

The grooves hollowed at the rotor surface permit to increase the active power without raising the reactive power, increase the reluctance of the magnetic circuit constituted by the iron along the groove and by the air through the notch and therefore, improve the performances of the motor. The grooves do not reduce the mechanical resistance of the rotor. They modify considerably the penetration of the magnetic flux inside the rotor and canalize the induced rotor currents [2],[4],[5]. Various works [4],[5],[6] have proposed to replace the grooved region by a smooth equivalent region. The operation of electrical motors depends upon the magnetic state of the magnetic core parts.

## 2 Theoretical Study

Many studies have been devoted to the determination of electrical machines performances such as the solid rotor asynchronous motors [2],[4],[5],[7]. The exhaustive study of the electromagnetic field diffusion in the solid rotor is very complex. The magnetic field penetrates to a certain depth in the rotor and induces Foucault's currents. These currents are not generated in definite conductors as in the classic motors (squirrel cage), but in a continuous environment that presents a non linear magnetic characteristic. Besides, these currents

close before reaching the rotor extremities. The diffusion of the electromagnetic field in the solid rotor is formulated by Maxwell's equations [4],[8],[9].

**2.1 Study models and general equations**

The rotor is characterized by a permeability  $\mu$  and a conductivity  $\sigma$ . When the rotor is subjected to a variable magnetic field, the distribution of the magnetic vector potential  $\vec{A}$  in the rotor obey to the Poisson equation:

$$\Delta \vec{A} = \mu \sigma \frac{d\vec{A}}{dt} \tag{1}$$

The distribution in the air gap obey to the Laplace's equation:

$$\Delta \vec{A} = 0 \tag{2}$$

The analysis of the solid rotor asynchronous machines behaviour leads to the solution of Maxwell's equations in a three-dimensional domain. This solution is extremely complex and some simplifying assumptions are then necessary to bring back the study in a bi-dimensional domain. The adopted simplifying hypothesis are :

- The permeability of the stator is infinite, the conductivity is neglected following the axis of the machine due to his folding.
- The stator coils is supplied by a three-phase currents equilibrium system of pulsation  $\omega$  with sinusoidal variation with the time
- The hysteresis phenomena is neglected.
- The machine axial length is infinite.
- The air gap is constant.

Considering these hypothesis, the study is brought back to a Cartesian reference frame  $(O,x,y,z)$  linked to the rotor as the  $Ox$  axis is radial and directed inside the machine, the  $Oy$  axis is tangent to the surface of the rotor and the axis  $Oz$  is parallel to the rotating axis. The origin  $O$  of the reference frame is placed on the surface of the rotor, in the middle of the length of this last. The theoretical model of the solid rotor machine is illustrated in figure1.

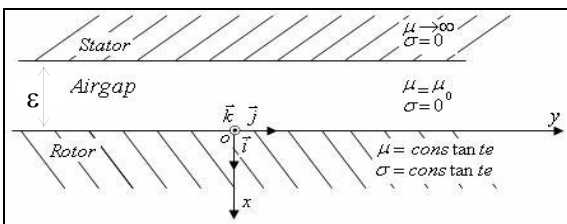


Fig.1 Theoretical model of the solid rotor machine

The magnetic vector potential is directed following

the  $Oz$ -axis and is independent of the  $z$  variable.

Therefore,  $\vec{A} = (0 \ 0 \ A_z(x, y, t))$

The study models of two types of rotors are shown in figure 2.

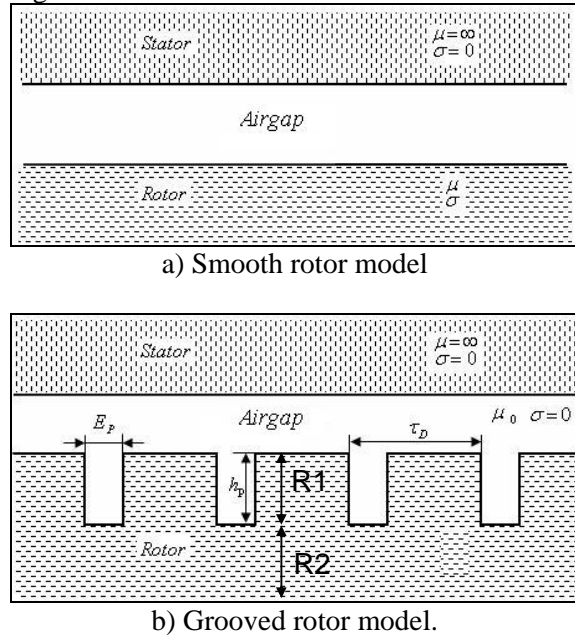


Fig.2 Study models of Smooth and Grooved rotors

$\epsilon, \epsilon_p, h_p$ : are respectively the air gap thickness, the groove width, and groove depth.

$$\tau_p = \frac{\pi D}{2p} \text{ : polar step.}$$

$$\tau_D = \frac{2\pi}{N_r} \text{ : dental step.}$$

$D$  : rotor diameter.  $p$  : number of pairs of poles.  $N_r$  : number of grooves.

R1: region 1 (anisotrope), in which:

$$B_{x_1} = \mu_{x_1} H_{x_1}, B_{y_1} = \mu_{y_1} H_{y_1} \text{ and } J_{z_1} = \sigma_{z_1} E_{z_1} .$$

R2: region 2 (isotrope), in which:

$$\mu_{y_2} = \mu_{x_2} = \mu_2 \text{ and } J_{z_2} = \sigma_2 E_{z_2} .$$

$B, H, J$  and  $E$  are respectively the magnetic induction, the magnetic field intensity, the current density and the electric field, in the regions 1 and 2, following  $x, y$  and  $z$ -axis.

The current superficial density  $J_s$  on the stator surface is given by the following relation:

$$J_s = \frac{3}{2} \frac{K_s}{\sqrt{2}} [I_1 e^{j\varphi} + I_1^* e^{-j\varphi}] \tag{3}$$

Where:

$$\varphi = a y + s \omega t$$

$$a = \frac{2\pi}{\tau_p} \text{ : Geometric rotor pulsation}$$

s : The slip

$I_1$ : current of a stator phase

$I_1^*$ : conjugate of  $I_1$ .

$K_s$ : Coefficient that takes into account the winding and the passage of the volume density of current to the equivalent superficial density.

- In the rotor :

$$\Delta \hat{A}^p(x, y, t) = \mu \sigma \frac{\partial \hat{A}^p}{\partial t}(x, y, t) \quad (4)$$

- And in the air gap :

$$\Delta \hat{A}^p(x, y, t) = 0 \quad (5)$$

The relation (5), determines the magnetic vector potential  $A_e$ , necessary to determine the magnetic flux  $\psi$  in the air gap. The expressions of the magnetic energy of the stator coils give:

$$\sum_{i=1}^3 \Phi_i(t) I_i(t) = \int_0^{2\pi p} A_e(x = -\varepsilon, \varphi) J_s L \frac{d\varphi}{a} \quad (6)$$

$\Phi_i(t)$ ,  $I_i(t)$  are the flux and the current of a phase.

L: length of the machine. From (6) :

$$\Psi = \sqrt{2} \pi \cdot p \cdot L \cdot \frac{K_s}{a} A_e(-\varepsilon) \quad (7)$$

The per-phase equivalent circuit of a solid rotor asynchronous motor is shown in figure 3.

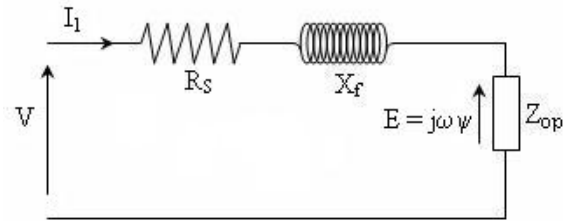


Fig.3 Per-phase equivalent circuit of solid rotor asynchronous motor

Where V,  $R_s$ ,  $X_f$ , E are respectively the supply voltage, the stator resistance, the leakage reactance, and back electromotive force.

From the equivalent circuit, the operational impedance  $Z_{OP}$  is given by :

$$Z_{op} = \frac{E}{I_1} = \frac{j\omega\Psi}{I_1} \quad (8)$$

- For the smooth rotor :

$$Z_{op} = j \frac{3}{2} \pi p \omega \mu_0 L \left[ \frac{K_s}{a} \right]^2 \frac{\text{ch}(a\varepsilon) + \frac{q}{\mu_r a} \text{sh}(a\varepsilon)}{\text{sh}(a\varepsilon) + \frac{q}{\mu_r a} \text{ch}(a\varepsilon)} \quad (9)$$

$$q^2 = a^2 + j\mu\sigma s\omega$$

- For the grooved rotor:

$$Z_{op} = j \frac{3}{2} \pi p \omega \mu_0 L \left[ \frac{K_s}{a} \right]^2 \left[ (\text{ch } a\varepsilon)^2 - 1 + F \right]$$

$$F = \frac{\text{ath } a\varepsilon (1 + k \text{th } q_1 h_p)}{\frac{\mu_0}{\mu_2} q_2 \left( 1 + \frac{1}{k} \text{th } q_1 h_p \right) + \text{ath } a\varepsilon (1 + k \text{th } q_1 h_p)} \quad (10)$$

$$k = \frac{\mu_{y1} q_2}{\mu_2 q_1}$$

$$q_1^2 = \mu_{y1} \left( \frac{a^2}{\mu_{x1}} + j\sigma_{z1} s\omega \right) \quad (11)$$

$$q_2^2 = a^2 + j\mu_2 \sigma_2 s\omega$$

The current of stator phase is given by :

$$I_1 = \frac{V}{R_s + \Re(Z_{op}) + j(X_f + \Im(Z_{op}))} \quad (12)$$

Where:  $\Re(Z_{op})$ ,  $\Im(Z_{op})$  are respectively the real and imaginary parts of  $Z_{op}$ ,

The electromagnetic torque is given by :

$$\Gamma = 3 \frac{P}{\omega} |I_1|^2 \Re(Z_{op}) \quad (13)$$

Using the equation (12), the electromagnetic torque becomes :

$$\Gamma = 3 \frac{P}{\omega} \frac{\Re(Z_{op})}{(R_s + \Re(Z_{op}))^2 + (X_f + \Im(Z_{op}))^2} V^2 \quad (14)$$

The Power factor is given by :

$$\cos \varphi = \frac{\Re(I_1)}{|I_1|} \quad (15)$$

### 3 Experimental Study

The experimental study consists of a series of tests realised on six (06) solid rotors (02 smooth and 04 grooved) of different configurations. The objective of this study is to examine the influence of the geometric parameter's solid rotor on the performances of solid rotor asynchronous motor. we will expose the experimental results by considering two essential parameters: the electromagnetic torque and the power factor.

The used motor's stator belongs to a classic asynchronous motor characterized by:

Power..... 7.5 kW  
 Rated voltage ( $\Delta/Y$ )..... 380/660 V.  
 Rated current ( $\Delta/Y$ )..... 15.5/8.9 A.  
 Connection..... star  
 Frequency..... 50 Hz.  
 Number of poles ..... 2  
 Diameter of stator..... 99 mm.  
 Number of stator slots... 24.

The tested solid rotors present the following characteristics :

Table 1 Dimensions of tested rotors

Rotor	D (mm)	L (mm)	$\epsilon$ (mm)	$E_p$ (mm)	$h_p$ (mm)	$N_r$
SR1	98	160	0.5	--	--	--
SR2	97	160	1	--	--	--
GR1	98	160	0.5	2.5	5	1 8
GR2	98	160	0.5	2.5	5	1 2
GR3	98	160	0.5	2.5	8	1 2
GR4	98	160	0.5	4	8	1 2

SR : smooth rotor, GR : grooved rotor.

### 3.1 Tests and results

For each rotor, a set of tests have been realised in load under a constant supply voltage. For different values of the supply voltage : the supply voltage, the power, the absorbed current, the torque, the power factor and the rotating speed are measured. For each rotor and for each supply voltage, the variations of the electromagnetic torque and the power factor versus the slip are drawn. Owing to space limitation, our discussion will be limited on a comparative study of the different characteristics for each rotor under a supply voltage of 500V and 300V. The same results have been obtained for supply voltage of (400 V and 200 V).

#### 3.1.1 Electromagnetic torque

The results show that the solid rotor asynchronous motor presents a good starting torque which deteriorates to the weak slips. For a given supply voltage, the electromagnetic torque developed by the solid rotor increases with the slip.

##### a. Influence of the air gap thickness

Figure 4 illustrates the influence of the air gap thickness on the electromagnetic torque characteristic of the smooth solid rotor

asynchronous motor. For the considered supply voltage, the SR1 present a better characteristics that those of the SR2.

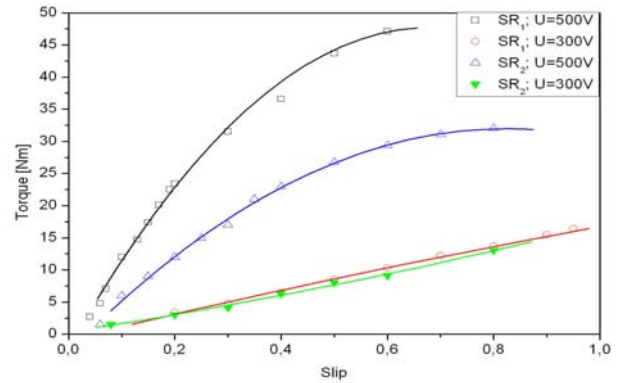


Fig.4 Influence of the air gap thickness

##### b. Influence of the grooves

Figure 5 depicts that for considered supply voltage, the electromagnetic torque developed by GR1 is distinctly better than the one of SR1 of the same diameter.

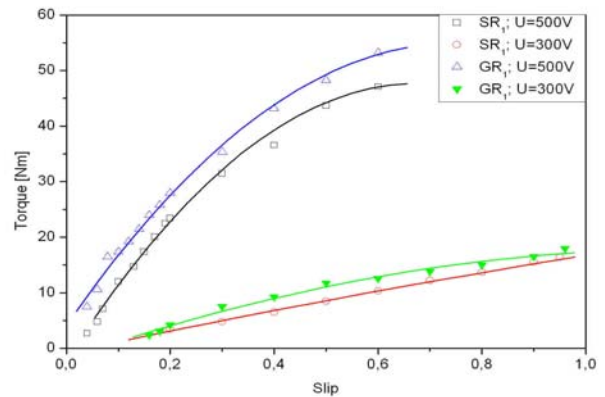


Fig.5 Influence of the grooves

##### c. Influence of grooves number

Figure 6 shows a comparison between the torque-slips characteristics of the two grooved rotors GR1 and GR2 for the used supply voltage. The rotor GR1 presents a better characteristic for all supply voltage.

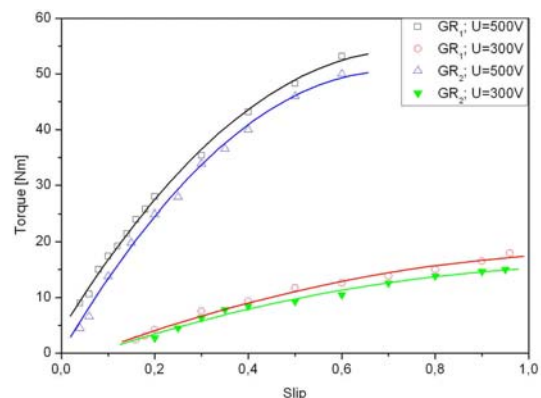


Fig.6 Influence of grooves number

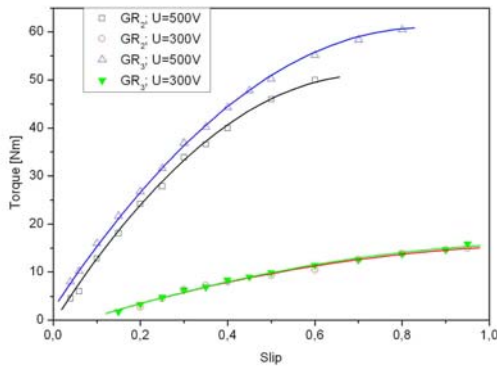


Fig.7 Influence of the grooves depth

**d. Influence of the grooves depth**

Figure 7 shows the torque-slips characteristics of the two grooved rotors GR2 and GR3, for two different supply voltage. The obtained results show that, for a given supply voltage, the torque-slip characteristic is much better when the grooves are deeper.

**e. Influence of the grooves width**

Figure 8 shows the torque-slips characteristics for two different values of supply voltage. The results show that, for the used supply voltage, two zones of variation of characteristics torque-slip are distinguished :

- For important slips ( $s > 60\%$ ), the GR4 provides a better characteristic.
- For weak slips ( $s < 60\%$ ), the GR3 develops the best electromagnetic torque.

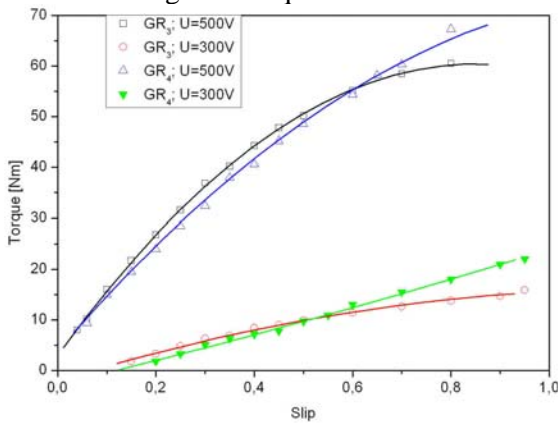


Fig.8 Influence of the grooves width.

**3.1.2 Power factor**

The power factor is the second greatness used to estimate the performances of the solid rotor asynchronous motor. The power factor versus slip characteristics are gotten for the different rotors. The characteristics show that the solid rotor

asynchronous motor present a good power factor during the starting then decreases appreciably for weak slips. For the used supply voltage, the power factor grows with the slip.

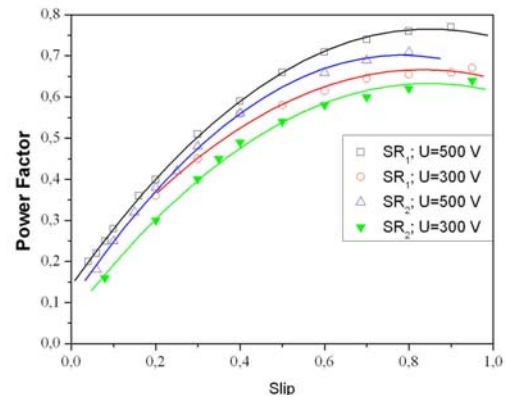


Fig.9 Influence of the air gap thickness

**a. Influence of the air gap thickness**

Figure 9 illustrates the characteristics of the power factor versus the slip for the two smooth rotors SR1 and SR2. For the used supply voltage, the power factor is better when the thickness of the air gap is weaker.

**b. Influence of the grooves**

Let us compare the characteristics of the tested rotors in order to determine the influence of the grooves on the power factor of the solid rotor motor. Figure 10 presents the compared characteristics of the rotors SR1 and GR1 of the same diameter. The comparison of the characteristics shows that the rotor GR1 presents a better characteristic than the one of the rotor SR1.

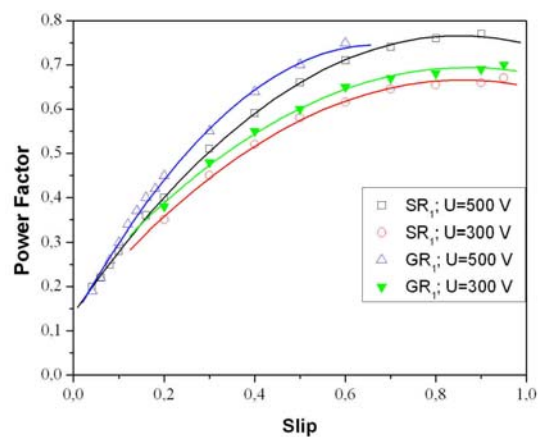


Fig.10 Influence of the grooves

**c. Influence of the grooves number**

In order to determine the effect of the number of grooves on the power factor of the solid rotor motor, the characteristics of the two rotors GR1 and GR2 have been drawn as shown in Fig.11. It appears that



the rotor GR1 has a bigger power factor than the one of the rotor GR2. For the used supply voltage, the rotor GR1 presents a better characteristic of the power factor in comparison to other tested rotors.

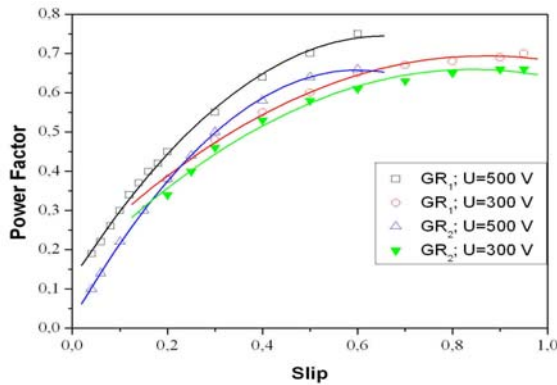


Fig.11 Influence of the grooves number

**d. Influence of the grooves depth**

The two tested rotors GR2 and GR3 have the same grooves number, but differ by the depth of their grooves. The characteristics power factor - slip are represented in figure 12. For weak slips ( $s < 40\%$ ), the characteristics of the two rotors are nearly confounded. For slips ( $s > 40\%$ ), the rotor GR3 offers the best power factor.

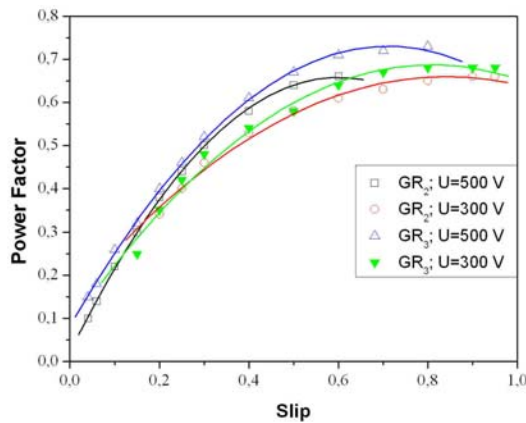


Fig.12 Influence of the grooves depth

**e. Influence of the grooves width**

The characteristics power factor - slip, for the rotors GR3 and GR4 are represented in figure 13. The rotor GR4 offers the best power factor.

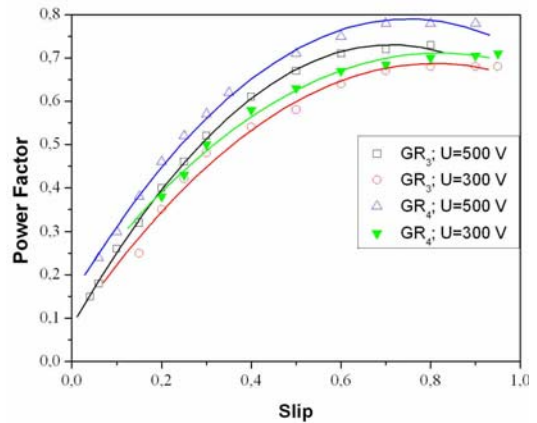


Fig.13 Influence of the grooves width

**4 Conclusion**

This paper presents experimental investigations conducted on six different solid rotors. The tests realised for different supply voltage, show the influence of the geometry of the solid rotor on the performances of the motor. The results have shown that the solid rotor asynchronous motor presents a good starting torque, and then deteriorates to the weak slips. The smooth solid rotor motor presents a better torque when the thickness of the air gap is weaker. Generally, the grooved rotor offers a bigger torque than the one of the smooth rotor. The different characteristics show that the solid rotor asynchronous motor has a good power factor during the starting, and then deteriorates to the weak slips. For a smooth solid rotor, the characteristics of the power factor versus the slip are much better when the air gap of the motor is smaller. The results show that the grooved solid rotor presents a better power factor than the smooth rotor. The power factor of the solid rotor motor increases with the supply voltage.

*References:*

- [1] P.K. Rajagopalan, V. Balarama Murty. Effects of Axial Slits on The Performance of Induction Machines With Solid Iron Rotors, *IEEE, Trans. PAS*, vol 88, N°11, Nov. 1969.
- [2] M.E Zaim, *Contribution à la conception des machines asynchrones à rotor massif*. Thèse de Doctorat de l'ENP Algiers (Algeria) 1989.
- [3] N.D Sharma, R. Anbarasy, J. Nataraj, A.Y Dangore, B. Bhattacharjee, Experimental Investigation on High Speed Solid and Composite Rotor Induction Motor. *Proc. of Int. Conf. On Power Electronics, Drives and Energy Systems for Ind. Growth*, vol.2, pp.913-919, Jan. 1996.

- [4] M. Ladjal, *Contribution à l'étude des moteurs asynchrones à rotor massif en vue de l'optimisation de leurs performances*, Thèse de magister, E.N.P Algiers, Algeria 1999.
- [5] J. M Biedinger, *Contribution A L'étude De La Diffusion Du Champ Electromagnétique Dans Le Fer Massif. Application A L'analyse D'un Moteur Asynchrone A Rotor Massif*. Thèse de Doctorat d'état, Université de Compiègne (France), Nov.1986
- [6] M.S Sarma, G.R Soni, Experimental Study of solid rotor and composite rotor Induction Motors. *IEEE. Trans. on Power Apparatus Systems*. Vol.91.No5.pp 1812-1820. 1972.
- [7] L. Changhong, Y. Ruoping A New Approach to Calculate Equivalent Circuit Parameters of the Induction Motor with Solid Rotor. *IEEE Int. IEMDC'03*, June 2003 vol.3, pp.1612-1615.
- [8] L.T. Ergene, S.J. Salon, One slot AC steady state model of a canned-solid rotor induction motor, *IEEE Trans. on Magnetics*.Vol.40, no.4, July 2004.
- [9] L.T. Ergene, S.J. Salon, Determining the Equivalent Circuit Parameters of Canned Solid Rotor Induction Motors, *IEEE Transactions on Magnetics*.Vol.41, no.7, July 2005.